

RESEARCH ARTICLE

Analysis and optimization of a solenoid coupler for wireless electric vehicle charging

KATHARINA KNAISCH, TOM HUCK AND PETER GRATZFELD

In light of the increased interest in e-mobility, comfortable, and safe charging systems, such as inductive charging systems, are gaining importance. Several standardization bodies develop guidelines and specifications for inductive power transfer systems in order to ensure a good interoperability between different coil architectures from the various car manufacturers, wireless power transfer suppliers, and infrastructure companies. A combination of a bipolar magnetic coil design on the primary side with a secondary solenoidal coil promises a good magnetic coupling and a high-transmitted power with small dimensions at the same time. In order to get a profound knowledge of the influence and behavior of the main variables on the coil system, a detailed parameter study is conducted in this paper. Based on these findings, a solenoid was designed for a specific case of application. Further, this design is optimized. The dimensions of the system could be reduced by 50% with a constant coupling factor at the same time. Besides the reduction of the dimensions and subsequently the costs of the systems, the stray field could be reduced significantly.

Keywords: Inductive power transfer, Electric vehicles, Coil design, Solenoid, Optimization

Received 18 May 2016; Revised 10 October 2016; Accepted 12 October 2016; first published online 22 November 2016

I. INTRODUCTION

In contrast to conductive charging systems, inductive power transfer (IPT) systems do not require a physical connection between the battery and the charging station. Therefore, inductive charging stations are much more comfortable and user friendly, especially during poor weather conditions. They are safe against vandalism as all devices are encapsulated in the vehicle and the ground. This is why IPT systems cover a broad range of application: they are used for charging portable devices, biomedical implants, vehicles, and much more. They find application for various power ranges and various air gaps [1, 2]. Stationary charging is further developed to dynamic charging where the vehicle is charged while it is actually moving [3, 4].

As IPT systems for charging electric vehicles (EVs) are increasing their market share, there also are various coupler topologies, which are deployed by the various car manufacturer, infrastructure companies, and wireless power transfer suppliers. In order to ensure a good interoperability between different coil topologies, there are several international and national standardization bodies, which focus on the specification of the components on the vehicle as well on the infrastructure side.

At present, standardization bodies contemplate a solenoid coil for the vehicle side, as it is a promising design. Compared with other topologies, a solenoid has a good coupling

coefficient with small dimensions at the same time. To date, however, there is little published information on the specific design of a solenoid for IPT EVs. Therefore, this study identifies the main variables on the coil system and highlights their impact on the system behavior. The aim of this work is to get a profound knowledge of the design and optimization of a solenoidal coil.

In the first part of this section, current literature and the current state of knowledge are analyzed. Furthermore, several national and international standardization bodies dealing with IPT systems for EVs are presented. The third part shortly explains the fundamentals of an IPT system. In Section II, the influence of the main geometric variables of a solenoidal coil is analyzed using parameter studies. Based on these findings a coil system is designed and optimized for a specific case of application in Section III. In Section IV, simulation results are validated and verified. Finally, Section V summarizes the findings and further areas of research are identified.

A) State of knowledge

Currently primarily three types of coupler topologies are applied in IPT applications for charging EVs: circular planar, bipolar, and solenoidal coils, as illustrated in Figure 1 [5].

They differ from each other mainly in the nature of their generated flux: a circular coil, as a nonpolarized coupler, generates a perpendicular flux, whereas DD coils or solenoids are polarized couplers, as they generate a parallel flux. Bipolar pads, which have mutually decoupled partially overlapping coils, can couple power from both the parallel flux and the perpendicular flux [6]. As bipolar pads are able to effectively

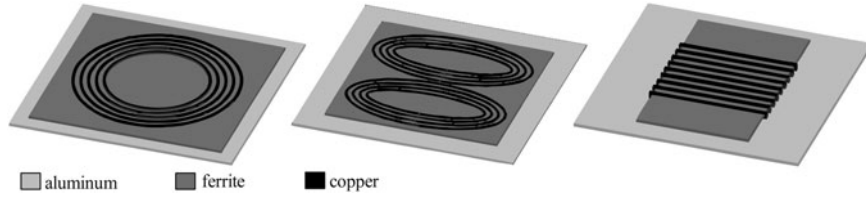


Fig. 1. Coupler topologies for IPT.

couple with various coil topologies, they are particularly suitable for an interoperable power transfer. Since the bipolar pad is known to interoperate with the other coil designs, the bipolar design is chosen in this study as a universal primary topology [1, 7]. Besides, the standard IEC 61980-3 also recommends the bipolar coil architecture as a primary topology [8].

On the secondary side, a solenoidal coil is chosen in this paper, as this architecture has a promising performance. It has a generally better coupling and smaller dimensions than other coupler topologies. However, the magnetic stray fields are relatively high [9]. The standard IEC 61980-3 also recommends, among others, a secondary solenoidal coil [8].

In order to exploit the full potential of the solenoid coil, an accurate magnetic design is indispensable. Nevertheless, to date there is little published information on the specific design of a solenoid for IPT of EVs.

Most studies focused on partial aspects of the coil design, as in [10–12], where specific cases of applications are assumed. Thus, the findings of these studies can be used for the design of other solenoids only to a limited extent. Hence, in this paper a comprehensive parameter study is conducted. All geometric variables are varied likewise and their influence on the entire output variables is examined. The aim of this work is to get a profound knowledge of the design and optimization of a solenoidal coil.

B) Standardization activities

In this section, the current standardization activities for IPT systems are presented. There are several international and national standardization bodies, such as ISO (PAS 19363), SAE (J2954), IEC (61980), and ICNIRP. ISO, SAE, and IEC categorize IPT systems according to several air gap classes and power transfer classes. In addition, they develop specifications for the components on the vehicle-side as well as on the infrastructure side.

Guidelines on the exposure to time-varying electric, magnetic, and electromagnetic fields are issued by the International Commission on Non-Ionizing Radiation Protection (ICNIRP). In order to protect against any known health effect, the exposure limit for the magnetic stray field of $27 \mu\text{T}$ for a frequency range of 3–10 MHz has to be met [13]. Previous ICNIRP guidelines from 1998 restrict the

magnetic stray field to $6.25 \mu\text{T}$ [14]. The main standardization bodies and their standards are summarized in Table 1.

C) Fundamentals of IPT systems

Figure 2 shows the main components of an IPT system. The primary system is fed by a primary AC source. Power electronics convert the low-frequency grid current into a high-frequency output current to feed the primary coil [15]. In loosely-coupled coils, such as the ones used in IPT, leakage inductances are large. Therefore, reactive power needs to be compensated in order to prevent further losses. This is done by compensating capacitors, which form resonant circuits with the coils [16]. The secondary part of the IPT system is composed similarly. In automotive applications, the secondary power converter usually consists of a rectifier and a chopper to feed the vehicle’s battery.

The output power of the system can be determined using the open-circuit voltage V_{oc} and the short-circuit current I_{sc} [17]:

$$P_{out} = I_{sc} \cdot V_{oc} \cdot Q_2. \quad (1)$$

The open-circuit voltage and the short-circuit current are calculated as follows:

$$V_{oc} = \omega \cdot M \cdot I_1, \quad (2)$$

$$I_{sc} = \frac{M}{L_2} \cdot I_1. \quad (3)$$

This leads to the following expression for the output power P_{out} :

$$P_{out} = \omega \cdot I_1^2 \cdot M^2 \cdot \frac{Q_2}{L_2}. \quad (4)$$

With the magnetic coupling coefficient k ,

$$k = \frac{M}{\sqrt{L_1 \cdot L_2}}, \quad (5)$$

Table 1. Standardization activities.

Standardization bodies	Standard	Main content
ISO (International Standardization Organization)	PAS 19363	Specification of charging topology
SAE (Society of Automotive Engineers)	J2954	Minimum performance and safety criteria
IEC (International Electrotechnical Commission)	61980	Specification of charging topology
ICNIRP (International Commission on Non-Ionizing Radiation Protection)	1998/2010	Exposure limits for magnetic fields

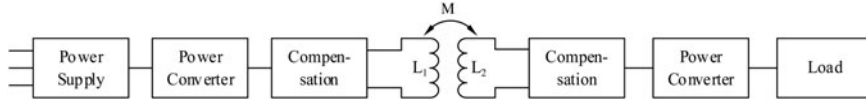


Fig. 2. Inductive power transfer system.

the output power can also be written as:

$$P_{out} = \omega \cdot L_1 \cdot I_1^2 \cdot Q_2 \cdot k^2. \quad (6)$$

As expression (6) shows, the output power can be increased by using a higher frequency, a larger primary current, or a higher quality factor Q_2 . Increasing the frequency is limited due to switching losses in power electronic devices. Using a larger primary current also results in larger copper losses. The quality factor of the coils is limited by manufacturing technology and costs. Therefore, the magnetic design has to be improved in order to increase the transferred power [17].

II. PARAMETER STUDY

A) System definition

Before defining the specific variables and their limits for the parameter study, the overall system with its input and output quantities is defined first, as illustrated in Fig. 3. Central elements of the parameter study are the primary

and the secondary coil with aluminum and ferrite plates. On the primary side a universal bipolar topology is used, which is kept constant for all simulations. The solenoid coil with a box-shaped ferrite core on the secondary side is examined in detail in this study. Other components, such as power electronic devices, are not part of the examination.

Input quantities of the system are the primary power input P_1 , the primary current I_1 , and the transfer frequency f . Output quantities are the secondary induced voltage U_2 as well as the secondary current I_2 . The input power is chosen to be 22 kW and the input current amounts to 85 A peak value. A fully compensated system is assumed. In order to be able to compare the various parameter settings, a constant transferred power is assumed. Thus, the secondary current is imposed accordingly.

Target values in this study are at one hand the self-inductances, the mutual inductance, and the coupling coefficient k . On the other hand, the magnetic field at the vehicle body has to meet the requirements of the ICNIRP guidelines. In order to take several vehicle types and their various widths into account, the magnetic flux density is evaluated at different distances and positions around the coils. Furthermore, size and weight of the coil system are a target value.

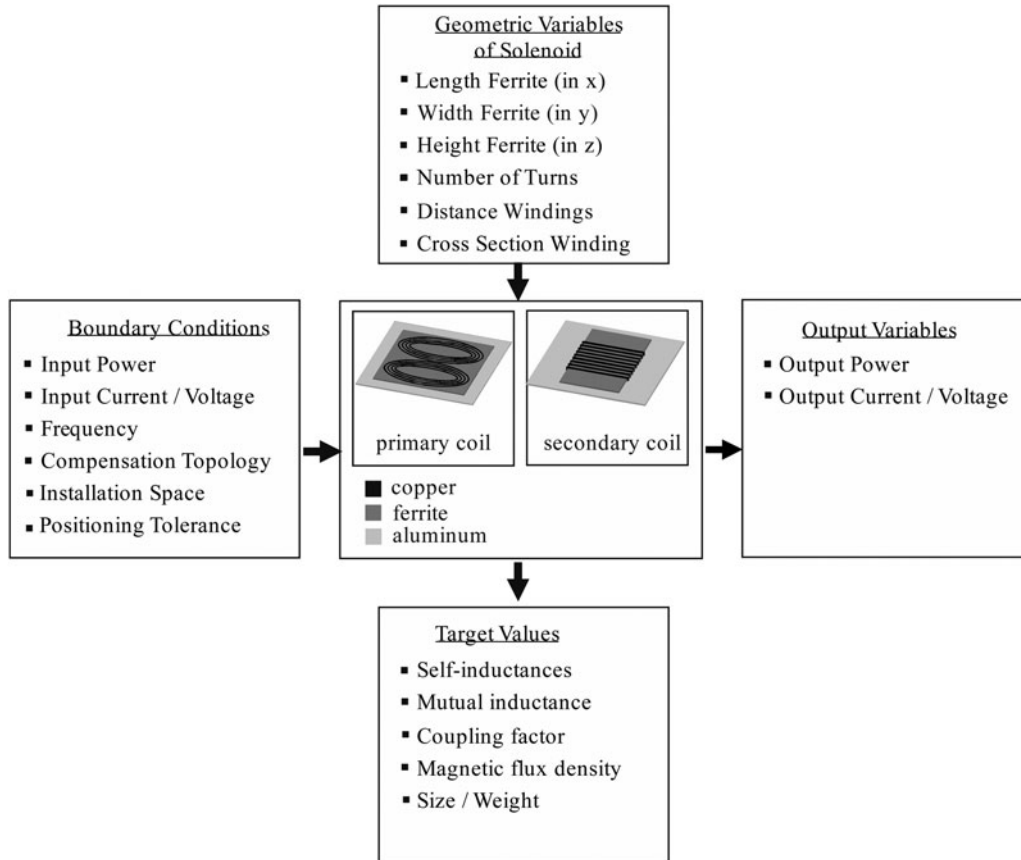


Fig. 3. System definition.

In order to analyze the positioning tolerance of the coil system, lateral displacements of 0–70 mm in the x -direction and 0–100 mm in the y -direction were taken into account.

All values are based on to the current state of technology and on the current requirements of the standardization bodies, see also Table 1.

B) Parameter study

As illustrated in Fig. 3, a bipolar pad is used as primary coil. The secondary coil, focus of this parameter study, is a solenoid with a box-shaped ferrite core. The range of the parameters varied also is listed in Fig. 4.

Each of the parameters of the secondary coil is simulated as a linear parametric sweep in ANSYS Maxwell, while the other parameters remain fixed. For each variation, the self- and mutual inductances as well as the magnetic coupling coefficient and the flux density values are calculated. The magnetic flux density is evaluated at three distances from the coil center: at 850, 1050, and 1250 mm. The smallest distance of 850 mm, as a worst case scenario, represents the vehicle body of a small car (e.g. a smart with a vehicle width of 1663 mm [18]). In order to take also larger vehicles into account, the magnetic flux density is calculated as well at distances of 1050 and 1250 mm.

The dimensions of the reference system and its target values are listed in Table 2.

C) Results of parameter study

In view of the extent of the results of the parameter study, only the most important results are discussed below. Table 3 gives a quantitative overview of the influence of the factors on the target values.

As the ferrite length in the x -direction increases, the flux pipe, dependent on the size of the ferrite, also gets larger. As it provides a path with less magnetic resistance, the self-inductance, as well as the flux density around the coil rises. The increase of the magnetic field in the x -direction is substantially larger than in the y -direction. Enlarging the ferrite in the y -dimension shows similar behavior, with an enlarged increase of the magnetic flux density in the y -direction. Overall effects of an enlargement of the ferrite height are generally not as strong as the effects of an enlargement in the x - or y -directions. Nevertheless, a moderate increase of the

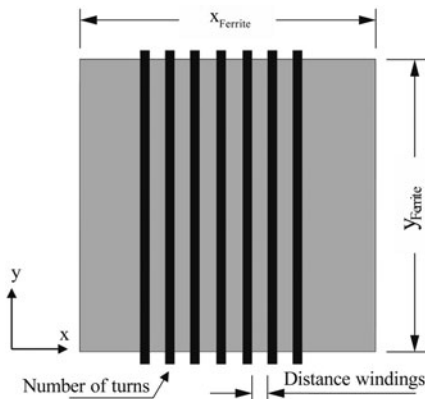


Fig. 4. Geometric parameters of the solenoid and their range.

Table 2. Dimensions and characteristics of the reference model.

Geometric variables		Target values	
Ferrite primary in x	750 mm	L_1	34 μ H
Ferrite primary in y	750 mm	L_2	32.6 μ H
Ferrite primary in z	5 mm	M	11.41 μ H
Number of turns primary	2×4	k	0.33
Distance windings primary	17 mm	$B_{x_850\text{mm}}$	19.79 μ T
Ferrite secondary in x	530 mm	$B_{x_1250\text{mm}}$	4.36 μ T
Ferrite secondary in y	530 mm	$B_{y_850\text{mm}}$	8.98 μ T
Ferrite secondary in z	5 mm	$B_{y_1250\text{mm}}$	2.14 μ T
Number of turns secondary	7		
Distance windings secondary	40 mm		

Table 3. Effects of the factors on the target values.

Increasing variable ...	Results in ...			
	L_2	k	B in x	B in y
X_{Ferrite}	↑	→	↑	↗
Y_{Ferrite}	↑	→	↗	↑
Z_{Ferrite}	↗	→	↗	↗
Number of turns	↑	→	↗	↗
Distance windings	↓	→	↗	↗
Cross-section winding	↘	↘	↗	↗

↑↘, considerable effect; ↗↘, moderate effect; →, marginal effect.

self-inductance as well as the flux density in both directions can be observed.

A large distance between the turns has a negative impact on the magnetic flux, as more flux passes between the windings. For this reason, the magnetic field in the surrounding of the coils increases. Moreover, the self-inductance decreases considerably.

The cross-sectional area of the litz wire also is under examination. Enlarging the cross-section results in a slight increase of the flux density. The self-inductance is reduced.

In the following optimization, however, the cross-sectional area is kept fixed as it is predominantly determined by the demanded ampacity.

Varying the factors, the coupling coefficient k shows a non-monotonic behavior, with different local maxima, depending on the factor's size. Only the factor of the conductor cross-section has a monotonic impact on the coupling factor.

Parameters	Range
X_{Ferrite} [mm]	300–700
Y_{Ferrite} [mm]	300–700
Z_{Ferrite} [mm]	2.5–20
Number of turns []	5–11
Distance windings [mm]	5–70
Cross section winding [mm ²]	50–800

Furthermore, the influence of a lateral misalignment on the IPT system is studied. As depicted in Fig. 5, it can be seen that a misalignment affects as well the coupling as the magnetic flux density on the vehicle body. In general, the system is much more sensitive to a misalignment in the x -direction than in the y -direction.

III. OPTIMIZATION

A) Approach

Based on the previous findings, the solenoid can now be optimized. The coupling factor shows local optima for various parameter settings. As there are strong interactions between the geometric variables, the main effects of the parameter study cannot be sensibly interpreted. In order to take the interaction effects between the factors into account, complex optimization algorithms are needed. However, because of the large number of variables the computational effort would be immensely high. Thus, a first iterative optimization, based on the main findings of the parameter study is conducted. In a second step, further room for improvement then is identified.

The main findings for the subsequent optimization are as follows:

- In order to reduce the magnetic flux density at the vehicle body the dimensions of the solenoid have to be decreased. Hereby, particular attention should be paid to the magnetic flux density in the y -direction, transversal to the driving direction. In the driving direction, the magnetic flux density at the vehicle body is well below the requirements of the ICNIRP guidelines.
- In order to adjust the inductances of the coils the number of windings and the distance between the windings can be varied. It is suggested first to regulate the number of windings for a coarse adjustment, as it only can be varied in discrete steps. A fine adjustment can be done by varying the distance of the windings.
- The distance of the windings shall be increased to a limited extent, as an enlarged distance affects the coupling factor and the magnetic stray field adversely.

These main findings lead to an iterative optimization approach.

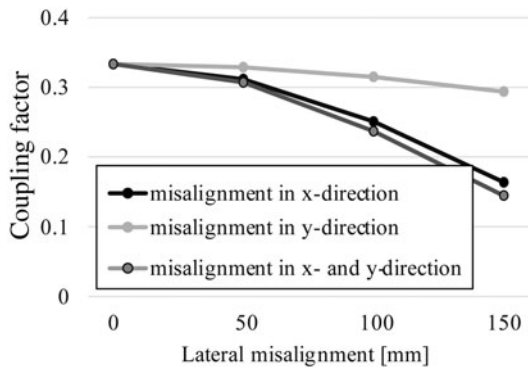


Fig. 5. Influence of a lateral misalignment.

Table 4. Optimization results.

Geometric variables of solenoid	Target values		
Ferrite in x	600 mm	L_1	34 μH
Ferrite in y	400 mm	L_2	33.7 μH
Ferrite in z	5 mm	M	12.09 μH
Number of turns	6	K	0.34
Distance windings	5 mm	$B_{x,850\text{mm}}$	18.6 μT
		$B_{x,1250\text{mm}}$	3.8 μT
		$B_{y,850\text{mm}}$	6.34 μT
		$B_{y,1250\text{mm}}$	1.63 μT
		k ($dx = 70$ mm, $dy = 0$ mm)	0.30
		k ($dx = 0$ mm, $dy = 100$ mm)	0.32

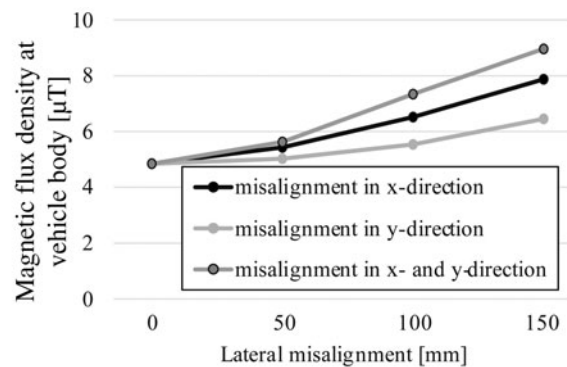
B) Optimization results

According to the previously described optimization approach, the optimized solenoid shows the following dimensions and target values, as listed in Table 4.

The length of the solenoid in the x -direction was increased from 530 to 600 mm, whereas the width in the y -direction decreased from 600 to 400 mm. The distance of the windings reduces from 40 to 5 mm. In order to attain a similar self-inductance compared with the reference system, the number of windings was slightly reduced from seven to six windings. Due to this optimization, the magnetic flux density could be significantly reduced: in the x -direction a decrease of 13% and in the y -direction a decrease of 30% could be noticed. Regarding the coupling factor the optimization results in an increased coupling factor under misalignment: in condition of an offset of 70 mm in the x -direction, the coupling factor can be increased from 0.28 to 0.30, in condition of a lateral misalignment of 100 mm, the coupling increases from 0.31 to 0.32. The coupling factor in nominal position only changes marginally to 0.34.

C) Weight minimization

The results of the previous optimization have shown that it is possible to reduce volume, weight, and flux density substantially without suffering from reductions of the coupling factor. These findings raise the question to which extent a



further reduction of size influences the coupling factor. For this reason, additional simulations were conducted.

With a constant width-to-length ratio of 1:1.5, the size of the ferrite was gradually decreased, while keeping the other parameters fixed. As Fig. 6 shows, the size of the solenoid can further be minimized to 300 mm × 450 mm without any substantial change of the coupling coefficient. Furthermore, the reduced size of the solenoid results in a decrease of the magnetic flux density. The magnetic field at the vehicle body was reduced by up to 36% in the x -direction and up to 46% in the y -direction. Volume and weight of the ferrite were reduced by more than 50%.

IV. VALIDATION AND VERIFICATION

As all results of this study are based on numerical simulations, they are only approximate simulations. In this section, the possible errors made are quantified. For the numerical simulation, there are two main steps: At first modeling the system and afterwards solving the differential equations. A validation ensures for the first step that the correct model is built and that the model is an accurate representation of the real model. For the second step, a verification estimates the deviation between the exact mathematical solution and the numerical approximated solution.

A) Verification

In order to quantify the quality of the numerical solution, several convergence criteria were defined. The mesh is refined adaptively until the specific convergence criteria are fulfilled. More precisely, a percentage energy error of 1% was defined as convergence criterion. Furthermore, the change of the inductances from one pass to another has to be smaller than 0.5%. In order to evaluate the quality of the numerical mesh in the surroundings of the coil system, the quality of the magnetic field was taken into account as well. For simulations with an axis of symmetry, the deviation of the magnetic field between the symmetrical planes was calculated. All simulations conducted in this study fulfill the defined convergence criteria to its full extent.

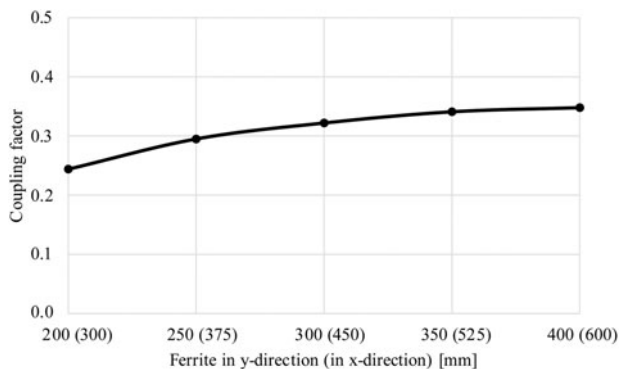


Fig. 6. Coupling factor when minimizing weight.

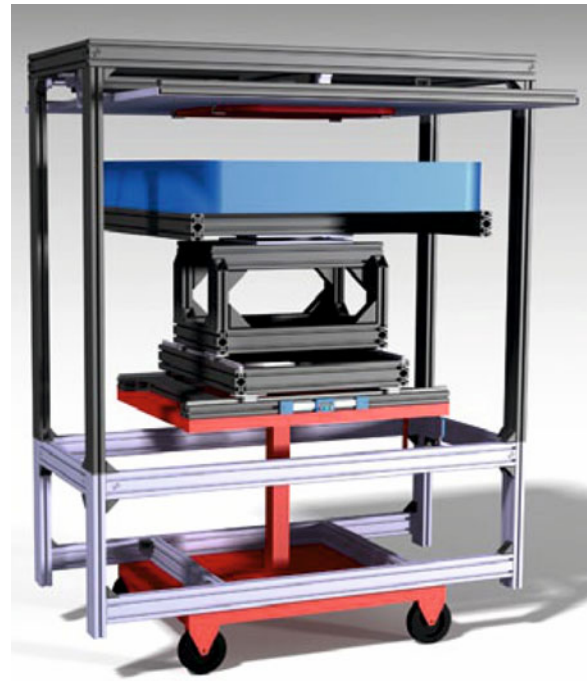


Fig. 7. 3D CAD model of the experimental prototype [19, 20].

B) Validation

For the estimation of the model error, simulation results were compared with the results of an experimental prototype, as shown in Fig. 7.

Due to reasons of complexity a prototype with circular planar coils was built, which fulfills the previously boundary conditions and requirements to its full extent. The dimensions of the experimental prototype are summarized in Table 5.

The existing simulation models were adapted accordingly and compared with the results of the experiments. For the measurements of inductances, 15 points were defined, which follow various lateral misalignments in the x - and y -directions (0, 25, 50, 75, and 100 mm) and various operational air gaps (120, 135, and 150 mm). The magnetic flux density also was measured and compared with the simulation results. As shown in Table 6, the averaged deviation between the measured and simulated results is well below 10%. The averaged absolute deviation of all measuring points is below 5%. It can be seen furthermore that the absolute deviation of all measuring points as well as the maximum deviation also are subject to a small error.

Table 5. Dimensions of the experimental prototype.

Geometric dimensions	
Coil diameter	510 mm
Number of turns	7
Cross-section of coil	50 mm ²
Distance between windings	13 mm
Ferrite on primary side	Ø 850 mm × 6 mm
Ferrite on secondary side	Ø 570 mm × 4 mm
Aluminum on primary side	Ø 940 mm × 5 mm
Aluminum on secondary side	Ø 600 mm × 5 mm

Table 6. Validation results.

Output variables	Results for reference model		Deviations simulations – measurements for all measuring points		
	Simulations	Measurement	Averaged (%)	Averaged absolute (%)	Maximum (%)
L_1	35.1 (μH)	36.9 (μH)	-4.04	5.17	4.94
L_2	34.4 (μH)	33.2 (μH)	3.80		4.47
K	0.34	0.32	7.67		8.82
B at vehicle body	8.1 (μT)	8.8 (μT)	-0.11	3.98	7.79

V. CONCLUSION

In this work, the influence of the main geometric variables of a solenoid was analyzed in detail. With a comprehensive parameter study, all geometric variables were varied likewise and their influence on the target values was examined. The most important geometric variables were identified and their specific influence on the behavior of the system was explained. Based on these findings, the coil system was then optimized. In a first approach, the coil size could be reduced by 17% with a constant coupling factor at the same time. In addition, the magnetic flux density at the vehicle body was reduced by 30%. A further optimization revealed that a further reduction in coil size is possible by more than 50% with an approximate constant coupling factor. The magnetic stray field at the vehicle body was reduced in this case by 46%. All simulations conducted in this study are validated and verified.

Further studies can be carried out to analyze and optimize the shielding of the coil system in order to meet the requirements of an adequate positioning tolerance. As a next step, an adapted experimental prototype is built and measured. Moreover, it is to show, to what extent these findings are applicable to other topologies. A comparison of several secondary topologies with a bipolar magnetic coil design on the primary side can highlight the specific advantages and disadvantages of each topology.

REFERENCES

- [1] Boys, J.T.; Covic, G.A.: IPT fact sheet series: no. 1 – basic concepts. (2016). Available: <https://www.qualcomm.com/media/documents/files/ippt-fact-sheet-1-uoa-2012.pdf>
- [2] Nagendra, G.R.; Covic, G.A.; Boys, J.T.: Determining the physical size of inductive couplers for IPT EV systems. *IEEE J. Emerg. Sel. Top. Power Electron.*, 2 (3) (2014), 571–583.
- [3] Lukic, S.; Pantic, Z.: Cutting the cord: static and dynamic inductive wireless charging of electric vehicles. *IEEE Electr. Mag.*, 1 (1) (2013), 57–64.
- [4] Vilathgamuwa, D.M.; Sampath, J.P.K.: Wireless power transfer (WPT) for electric vehicles (EVs) – present and future trends. *Plug In Electric Vehicles in Smart Grids*, Springer Science+Business Media Singapore, 33–60.
- [5] Li, S.; Mi, C.: Wireless power transfer for electric vehicle applications. *IEEE J. Emerg. Sel. Top. Power Electron.*, 3 (1) (2015), 4–17.
- [6] Zaheer, A.; Hao, H.; Covic, G.A.; Kacprzak, D.: Investigation of multiple decoupled coil primary pad topologies in lumped IPT systems for interoperable electric vehicle charging. *IEEE Trans. Power Electron.*, 30 (4) (2015), 1937–1955.
- [7] Lin, F.Y.; Zaheer, A.; Budhia, M.; Covic, G.A.: Reducing leakage flux in IPT systems by modifying pad ferrite structures, in *IEEE Energy Conversion Congress and Exposition (ECCE)*, 2014, 1770–1777.
- [8] IEC. Electric vehicle wireless power transfer (WPT) systems – Part 3: specific requirements for the magnetic field wireless power transfer systems: IEC 69/321/CD – IEC 61980-3/Ed.1. DKE Deutsche Kommission Elektrotechnik Elektronik Informationstechnik in DIN und VDE, 2014.
- [9] Ombach, G.; Kürschner, D.; Mathar, S.; Chlebosz, W.: Optimum magnetic solution for interoperable system for stationary wireless EV charging, in *Ecological Vehicles and Renewable Energies Conference in Monaco (EVER)*, 2015, 1–8.
- [10] Tang, Y.; Zhu, F.; Wang, Y.; Ma, H.: Design and optimizations of solenoid magnetic structure for inductive power transfer in EV applications. *Industrial Electronics Society*, 2015, 1459–1464, <http://ieeexplore.ieee.org/stamp/stamp.jsp?arnumber=7392306>.
- [11] Budhia, M.; Covic, G.A.; Boys, J.T.: A new IPT magnetic coupler for electric vehicle charging systems. *IEEE Industrial Electronics (IECON)*, 2010, 2487–2492.
- [12] Huang, C.-Y.: Design of IPT EV battery charging systems for variable coupling applications. PhD Thesis, University of Auckland, 2011.
- [13] ICNIRP – International Commission on Non-Ionizing Radiation Protection: Guidelines for limiting exposure to time-varying electric and magnetic fields (1 Hz – 100 kHz), 2010.
- [14] ICNIRP – International Commission on Non-Ionizing Radiation Protection: Guidelines for limiting exposure to time-varying electric, magnetic, and electromagnetic fields (up to 300 GHz), 1998.
- [15] Fisher, T.M.; Farley, K.B.; Gao, Y.; Bai, H.; Tse, Z.T.H.: Electric vehicle wireless charging technology: a state-of-the-art review of magnetic coupling systems. *Wireless Power Transf.*, 1 (2) (2014), 87–96.
- [16] Trevisan, R.; Costanzo, A.: State-of-the-art of contactless energy transfer (CET) systems: design rules and applications. *Wireless Power Transf.*, 1 (01) (2014), 10–20.
- [17] Boys, J.T.; Covic, G.A.: The inductive power transfer story at the University of Auckland. *IEEE Circuits Syst. Mag.*, 15 (2) (2015), 6–27.
- [18] Smart fortwo – technical data. Available: <https://www.smart.com/en/en/index/smart-fortwo-453/technical-data.html> (2016).
- [19] Baier, K.; Ehrentraut, P.: BIPoLPLUS -Kabelloses Laden mit 22kW. *ATZ extra.*, 11 (2014), 30–36.
- [20] Mayer, B.: Thermische Absicherung und Wirkungsgradtests beim induktiven Laden, in *5th Conference on Future Automotive Technology in Fürstenfeld*, May, 2016.



Katharina Knaisch received her Mechanical Engineering diploma in 2013 from the Karlsruhe Institute of Technology (KIT). She now is a Ph.D. student at the Institute of Vehicle System Technology at the KIT. Her research areas include the design and optimization of coil topologies for inductive power transfer for electric vehicles with high power.



Tom Huck studied mechatronics at the Karlsruhe Institute of Technology (KIT). In his bachelor thesis, he analyzed coil designs for inductive power transfer. After his current internship at the Department of e-mobility at Schaeffler Group, he will aim for the master's degree in Electrical Engineering.



Peter Gratzfeld is a full Professor at the Institute of Vehicle System Technology at the Karlsruhe Institute of Technology (KIT). He received his Ph.D. degree in Electrical Engineering from the RWTH Aachen University. From 1986 to 2008, he held several leading positions within the rail industry at Bombardier Transportation and its predecessor companies.